Levy, D. B., Custis, K. H., Casey, W. H. & Rock, P. A. (1997): The aqueous geochemistry of the abandoned Spenceville copper Pit, Nevada County, California. – J. Environ. Qual., 26 (1): 233-243, 3 Abb., 4 Tab.; Madison.

The Aqueous Geochemistry of the Abandoned Spenceville Copper Pit, Nevada County, California

D. B. Levy,* K. H. Custis, W. H. Casey, and P. A. Rock

ABSTRACT

The Spenceville Pit in Nevada County, CA, has been filled with acidic mine drainage for approximately 75 yr and is an active source of acidity and trace metals to an adjacent stream. This study was conducted to characterize the aqueous chemistry of the Spenceville Pit to better understand pit lake geochemistry. Filtered samples were collected at regular depth intervals and analyzed for Ca, Mg, Na, K, Fe, Al, Mn, Cu, Zn, Ba, Si, Pb, and P. The geochemical speciation model MINTEQA2 was used to calculate the activity ratios of Fe^{2+}(aq) to Fe^{3+}(aq) based on measurement of oxidation-reduction potential using a combination Pt/Ag-AgCl electrode, and to calculate saturation indices for various mineral phases. Sampling of the Spenceville Pit in summer (August) and in winter (December) shows that the deeper waters exhibit considerably higher concentrations of metals compared with the shallow waters, and that the water column may be permanently stratified. Neither the scavenging of trace metals (Cu, Ni, and Zn) by particulate iron-hydroxide minerals nor their precipitation as metal sulfides exerts significant control on the distribution of metals in the pit water. Instead, elemental distributions appear to be controlled by the process of cyclic filling and evaporation. Analysis of mineral saturation states in the pit water and x-ray diffraction analysis of the bottom sediments indicate that gypsum ($CaSO_4 \cdot 2H_2O$), goethite (α-FeOOH), jarosite [$KFe_3(SO_4)_2(OH)_6$], jurbanite ($AlOHSO_4 \cdot 5H_2O$), and strengite ($FePO_4 \cdot 2H_2O$) are solids that may potentially control elemental concentrations in the water column.

EXISTING PIT MINE LAKES in the western USA pose potential threats to local ground and surface water quality. In the state of Nevada alone, more than 30 pit mine lakes with the capacity to hold a total of approximately 1.2×10^{12} L of water will begin to form during the next 20 yr as groundwater flows into abandoned open pits (Miller et al., 1996). The water quality of existing pit lakes is highly variable and generally reflects the mineralogical composition of the pit wall rock. For example, the Cortez Mine (Cortez, NV) was a carbonate-hosted metal mine that began filling with water in the mid-1970s. The Cortez Pit contains good quality water, exhibiting a pH of approximately 8.0, and has concentrations of trace metals (e.g., Cu, Cd, Pb, and Zn) and total dissolved solids that meet applicable drinking water standards (Bird et al., 1994; Miller et al., 1996). In contrast, the Berkeley Pit (Butte, MT) contains acidic water (pH $\approx$ 3.0) that results from the oxidation of pyrite (FeS_2) and other metal sulfides. The concentrations of trace metals and total dissolved solids in the Berkeley Pit are significantly elevated and potentially toxic to aquatic life (Davis and Ashenberg, 1989; Miller et al., 1996). In addition to pit wall mineralogy, the overall water balance of pit lakes is another important factor controlling the water quality of pit lakes.

In recent years, it has been recognized that circulation patterns in pit lakes may affect observed depth distributions of dissolved O_2(g) and other constituents in the water column. The relative depth of the pit lake, or the ratio of the maximum depth as a percentage of the mean diameter of the lake at the surface (Wetzel, 1983), is one of the most important physical factors affecting the degree of seasonal turnover caused by the mixing action of winds. Hence, the relative depth of a pit lake affects the depth distributions of dissolved constituents (Lyons et al., 1994; Miller et al., 1996). In a recent study of pit lake limnology (Doyle, 1996), two shallow pit lakes (25 and 55 m deep) were observed to undergo seasonal turnover of the entire water column, while deeper pit lakes (110 and 130 m) exhibited seasonal turnover only of the upper portion of the water column. The extent of pit lake turnover is especially important because of its potential role in affecting the depth distributions of redox-sensitive elements (e.g., Fe, As, and Cr) in the water column.

The majority of pit lakes in North America are less than 25 yr old (Miller et al., 1996). The increasing number of pit lakes has prompted studies to determine the geochemical processes controlling metal transport in these settings. An understanding of these processes is required to provide a basis for predicting the water quality of future pit lakes and to assess environmental risks (Pillard et al., 1996; Lyons et al., 1994). The objectives of the present study were to (i) determine the chemical composition of water samples collected from various depths in the Spenceville Pit, (ii) identify the dominant geochemical processes that control metals concentrations in the water column, and (iii) discuss the role of seasonal variation relative to chemical compositions and stratification within the pit lake waters. The results of this study provide additional information on metals distributions within the water column of pit lakes. The results also show that certain geochemical and limnological processes that control metal concentrations and distributions within the water column of acidic pit lakes are analogous to those that operate in higher pH, natural lakes.

SITE DESCRIPTION

Approximately 2.3×10^7 L of acidic, metalliferous water occupies an open pit at the abandoned Spenceville Cu Mine in southwestern Nevada County, CA. The Spenceville Mine was initially operated by the San Fran-

D.B. Levy, Shepherd Miller Inc., 3801 Automation Way, Fort Collins, CO 80525; K.H. Custis, Office of Mine Reclamation, Dep. of Conservation, 801 K Street, Sacramento, CA 95814; W.H. Casey, Dep. of Land, Air, and Water Resources and Dep. of Geology, Univ. of California, Davis, CA 95616; and P.A. Rock, Dep. of Chemistry, Univ. of California, Davis, CA 95616. Received 18 Mar. 1996. *Corresponding author (dlevy@shepmill.com).

Published in J. Environ. Qual. 26:233–243 (1997).

Abbreviations: PVC, polyvinyl chloride; ICP-AES, inductively coupled plasma-atomic emission spectrometry; DOC, dissolved organic carbon; SHE, standard hydrogen electrode; SI, saturation index; XRD, x-ray diffraction.

cisco Copper Company between 1875 and 1888, when approximately 140 000 Mg of pyrite ore containing 5% Cu were excavated (Bradley, 1930). The principle sulfide minerals were chalcopyrite ($CuFeS_2$) and pyrite (FeS_2), and the ore deposit occurred as a continuous vein approximately 91 m long and 5 to 17 m wide. When the underground mine collapsed, mining was continued in an open cut (Fig. 1a) that was exposed to a length of 90 m and a depth of 23 m (Aubury, 1908). Mining operations ceased in 1888 owing to a fall in the price of Cu, and in 1890 the Imperial Paint and Copper Company established a furnace and paint mill on the property, where red-metallic (Fe_2O_3) paint was manufactured from the abandoned, roasted ore heaps (Bradley, 1930). In 1897, the property was acquired by the Spence Mineral Company, which reopened and dewatered the collapsed mine workings before the extraction of low-grade pyritic ore, that was used to manufacture sulfuric acid. Production operations finally ceased at the Spenceville Mine between 1916 and 1918 (Bradley, 1930), and the pit was subsequently flooded as a result of groundwater seepage and surface runoff (Fig. 1b).

The Spenceville Pit is 77 m long and approximately 28 m wide (Fig. 2). When filled to a water surface elevation of 102 m, the pit has a surface area of 2.0×10^3 m^2, a total volume of 2.3×10^7 L, and a maximum depth of 17 m. The relative depth of the Spenceville Pit is 34%. In comparison, the Berkeley Pit at Butte, MT, is approximately 1.8 km long and 1.4 km wide, was excavated to a depth of 542 m, and exhibits a fairly similar relative depth of 30% (Davis and Ashenberg, 1989). Although small in comparison, the Spenceville Pit is a significant source of localized surface water contamination. In winter, the pit becomes completely filled with water and overflows into Little Dry Creek. In summer, water continues to move laterally into Little Dry Creek through Eocene iron-oxide cemented terrace deposits, which overlie the metavolcanic bedrock (Fig. 1a).

MATERIALS AND METHODS

Water Sampling and Analytical Methods

The water column of the Spenceville Pit was sampled at two locations (Fig. 2) on 31 Aug. 1994 (summer) and on 28 Dec. 1994 (winter). At Sampling Station A, water samples were collected from the 0.3-, 1-, 2-, 3-, 4-, 8-, and 9-m depths. At Sampling Station B, water samples were collected from the 0.3-, 1-, 2-, 3-, 4-, 8-, 10-, and 15-m depths; an additional sample was collected at the 12-m depth during the winter sampling. Immediately before sampling, in situ measurements of pH, specific conductance, temperature, and dissolved O_2(g) were made with an Aqua Check Model 51601 Portable Water Analyzer extended to depth. The instrument was calibrated using standard solutions, and the readings were automatically corrected for the effects of temperature, pressure, and salinity. The flux of photosynthetically active radiation (400–700 nm) was measured at all depths with a Li-COR LI-192SA underwater quantum sensor. Approximately 2 L of sample were collected with a cylindrical, horizontal polyvinyl chloride (PVC) bottle equipped with a stainless steel split-barrel messenger. One-hundred mL of sample were filtered through a 0.20-μm pore-size polycarbonate membrane filter into a 250-mL, acid-washed polypropylene bottle. The samples were then acidified with high-purity nitric acid to a pH of approximately 1.0 and placed on ice for transport to the laboratory. The filtered, acidified samples were stored in the dark at 4°C for no more than 2 wk before determination of total dissolved Ca, Mg, Na, K, Fe, Al, Mn, Cu, Pb, Zn, Ba, Si, and P using inductively coupled plasma atomic emission spectrometry (ICP-AES) (APHA, 1992). The concentration of SO_4, as S, was determined by the ICP method described by Raue et al. (1991). A filtered, nonacidified 30-mL subsample was collected at the same time and stored on ice for analysis of dissolved organic carbon (DOC) using a Shimadzu TOC-5050 carbon analyzer. Element detection limits were calculated as three times the standard deviation of a nitric acid blank (pH = 2) that was filtered in the field using laboratory deionized–distilled water. Measured precisions for all analytes were ≤5% based on analysis of standard solutions, and charge imbalances calculated for the speciated solutions using the geochemical speciation model MINTEQA2 (USEPA, 1991) were ≤8%.

The oxidation–reduction potential (Eh) was measured immediately upon retrieval of the sample using a combination Pt/Ag–AgCl electrode, and the results were used to calculate the activity ratios of Fe^{2+}(aq) to Fe^{3+}(aq) in the water samples. The calculations were performed using the chemical equilibrium model MINTEQA2 (USEPA, 1991). The Pt electrode was immersed in a 250-mL subsample, and a stable reading was obtained within 2 min. Exposure of the sample to air during this time did not affect the measured Eh readings, and this was confirmed by monitoring the solution Eh of a sample of Spenceville sediment pore water collected without head space as it was purged with pure O_2(g) for 20 min in the laboratory. A stable Eh reading of 300 mV (not normalized to the Standard Hydrogen Electrode, SHE) was maintained for at least 20 min, and thus the oxidation rate of Fe^{2+}(aq) was shown to be too slow to be detected in the measured Eh readings. These observations are in agreement with previous studies that have shown that in acidic, iron-rich solutions, the measured Eh is a valid indicator of the redox status of the water and is not affected by presence of dissolved O_2(g) (Singer and Stumm, 1970; Sung and Morgan, 1980; D.D. Runnells et al., 1993, unpublished). Supporting studies have shown that the use of a Pt electrode is a valid method for determining Eh, and thus the activity ratio of Fe^{2+}(aq) to Fe^{3+}(aq) in acidic, iron-rich water, such as the water in the Spenceville Pit (Nordstrom et al., 1979; Ball and Nordstrom, 1985; Davis and Ashenberg, 1989; Levy et al., 1997). Oxidation of ferrous Fe is very slow (hours to days) in acidic waters, but the measurements in this study were made immediately upon sampling to further ensure that no change in Eh had occurred. The Eh measurements reported here were standardized relative to the SHE using Zobell's Solution (APHA, 1992).

Total suspended solids were measured on water samples from the winter sampling. Approximately 700 mL of sample were collected in 250-mL polypropylene bottles and cooled with ice. Within 24 h, the samples were filtered through dried (70°C for 3 h) polycarbonate-membrane filters (0.20 μm). Following filtration of the sample, the filters were dried (70°C for 3 h), reweighed, and the concentration of suspended solids was calculated by dividing the mass of suspended solid by the volume of water filtered.

Total sulfide was measured on location at all depths during the summer sampling utilizing the methylene-blue method (APHA, 1992) and a portable spectrophotometer. Based on the results of these measurements, sulfide analyses on waters collected during the subsequent winter sampling were carried out utilizing the Orion Model 94-16 Ag/Ag_2S electrode to gain higher sensitivity. These analyses were accomplished by

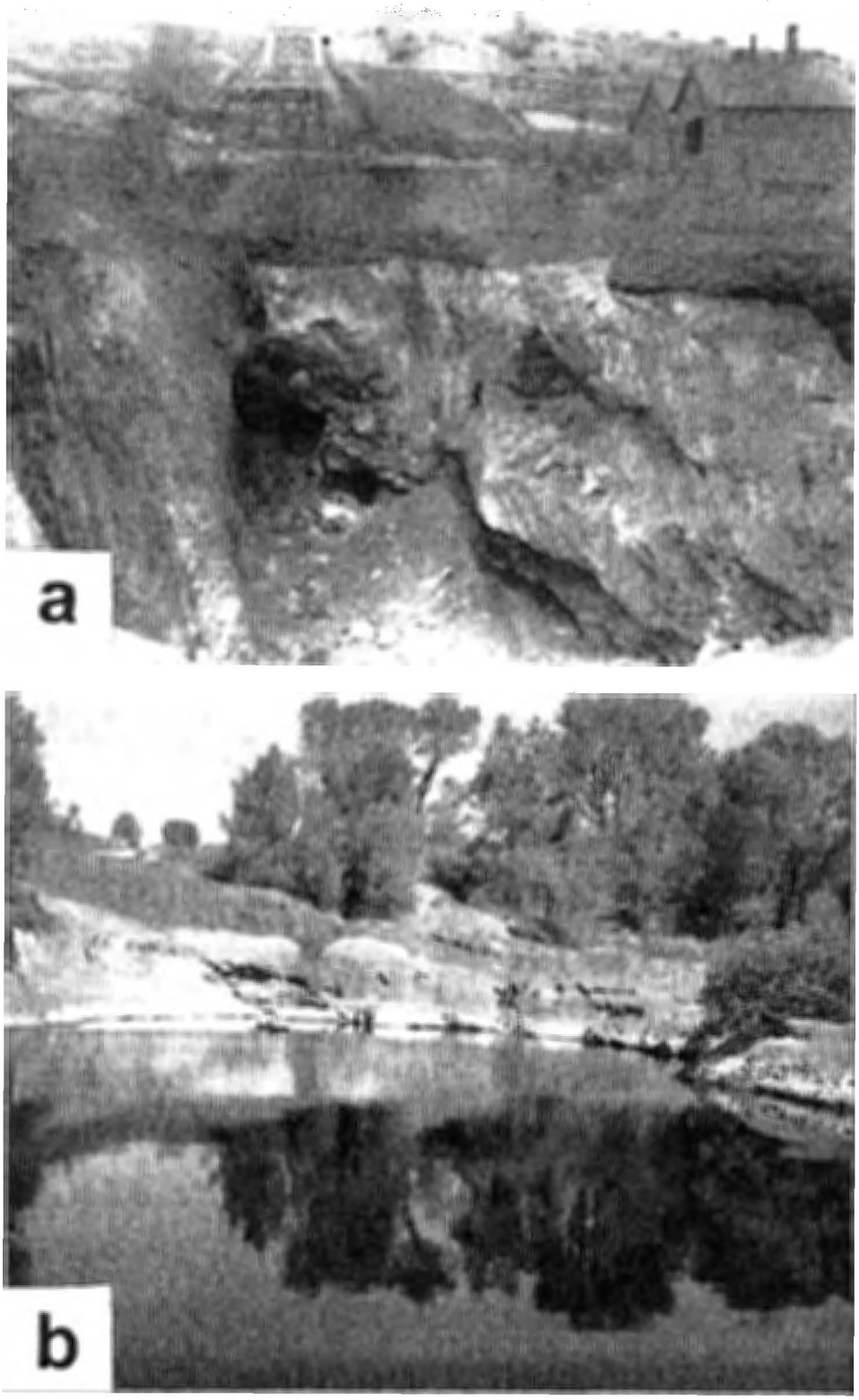

Fig. 1. (*a*) The Imperial Paint and Copper Co., about 1890. The large excavation was left by the San Francisco Copper Co., which operated the mine from 1875 to 1888. (*b*) The abandoned Spenceville Mine in 1994. Note the Fe-oxide cemented terrace deposits (*a*), overlying the metavolcanic bedrock, that transport dissolved metals and acidity to adjacent Little Dry Creek.

mixing 15 mL of sample with 15 mL of sulfide antioxidant buffer (NaOH + ascorbic acid) immediately upon sampling, and by placing the samples on ice to prevent oxidation of sulfides during transport to the laboratory. Dissolved sulfide was then measured with the Ag/Ag_2S electrode in the laboratory within 24 h.

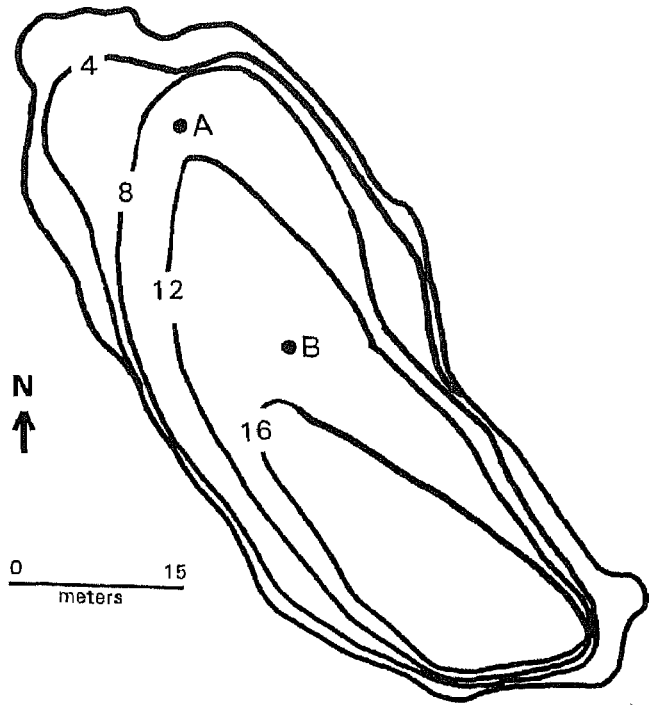

Fig. 2. Bathymetry of the Spenceville Pit showing Sampling Stations A and B.

To identify potential precipitation reactions that may act to control metal concentrations in the pit water, the saturation index (SI) for solids was calculated by MINTEQA2 using the equation:

$$SI = \log (IAP/K_{sp}) \quad [1]$$

where IAP is the ion activity product observed in solution, and K_{sp} is the theoretical solubility constant at the field temperature. Thus, a positive SI indicates that the solution is oversaturated with respect to a given solid phase, while a negative SI indicates undersaturation. A condition of oversaturation indicates that the precipitation of the respective mineral phase is thermodynamically possible. At SI = 0, the solution and the solid phase(s) being considered are in apparent equilibrium. In this study, apparent equilibrium was defined when the SI value for any solid phase under consideration was between −0.50 and +0.50, due to the inherent uncertainties in the analytical and thermodynamic data.

Sediment Sampling and Mineralogical Methods

Sediment from the pit lake floor was collected in winter with a spring-loaded box-type sampler and stored in 500-mL polyethylene bottles without head space at 4°C during transport to the laboratory. Samples of the sediments were centrifuged at 12 000 *g* for 20 min, and the Eh, pH, and sulfide concentrations of the extracted interstitial water were measured as described above. An aliquot of the supernatant liquid was filtered through a 0.20-μm pore-size filter and acidified with high-purity nitric acid for dissolved metal analysis by ICP. Triplicate samples of the sediment were digested for total elemental analysis (Lim and Jackson, 1982), and the amount of entrained pore water in the sample was calculated from a moisture determination. Total sediment metal concentrations were corrected for metals present in the entrained pore water by subtracting the mass of metal entrained in each sample.

The mineralogical composition of the sediment was determined by preparing a sample of the wet sediment as a paste mount (Theisen and Harward, 1962) followed by x-ray diffraction (XRD) analysis. For comparison, an air-dried sample (<2 mm) of the adjacent mine tailings, the dominant source of sediment to the pit, was analyzed by XRD as a random powder mount (Jackson, 1979). The samples were analyzed with a Scintag XDS-2000 diffractometer using Cu-Kα radiation with a Ge solid-state detector and calibrated to better than 0.01 degrees 2-theta using a corundum (α-Al_2O_3) standard. Mineral phases were identified with XRD by calculating distances between diffraction planes from the recorded diffraction peaks and comparing them with reference standards (Joint Comm. on Powder Diffr. Stand., 1993).

Water Balance Calculations

A water balance calculation was performed for the Spenceville Pit to estimate the amount of time that was required for pit filling after mining operations had ceased. The water balance consists of three inflow elements and four outflow elements. Inflow consists of (i) surface runoff during storms, (ii) precipitation onto the pond surface, and (iii) groundwater inflow through the metavolcanic bedrock. Outflow consists of (i) surface water overflow from the pit when it becomes filled, (ii) evaporation from the pond surface, (iii) groundwater outflow through the metavolcanic bedrock, and (iv) groundwater outflow through the terrace deposits when the pit becomes filled. The water balance was calculated on a monthly basis using a computer spreadsheet. Surface water runoff was calculated using methods described by the Soil Conservation Service (Haan et al., 1994), and evaporation rates were estimated from the tabulated evapotranspiration coefficients provided by Pruitt and Snyder (1985). Average monthly precipitation values were obtained from records of the California Department of Water Resources (1981). Monthly groundwater inflow through bedrock was calculated using Darcy's Law, assuming that the thickness of the bedrock aquifer (15 m) and the hydraulic gradient (0.066) remains constant, and using an average hydraulic conductivity of approximately 4×10^{-5} cm s^{-1} (S.S. Papadopulos and Associates, 1988, unpublished).

RESULTS

Chemistry of the Water Column

The specific conductance profiles show that the Spenceville Pit is chemically stratified (Fig. 3a). The conductance values were nearly constant in the upper 3 m (Locations A and B) and a stagnant water mass of higher salinity was identified between the 10- and 15-m depths (Location B). The two water masses are separated by a zone exhibiting an abrupt increase in salinity. In natural lakes that are permanently stratified (meromictic lakes), these zones are referred to as the mixolimnion, chemocline, and the monimolimnion, respectively (Wetzel, 1983); for convenience, we have adopted this terminology in the discussion of pit-lake stratification.

In summer, the specific conductance values ranged from 3.51 dS m^{-1} at the surface to 13.1 dS m^{-1} at the monimolimnion. In winter, the specific conductance values in the monimolimnion were comparable (12.8 dS m^{-1}), but the specific conductance values at the surface were lower in winter compared with summer (1.25 dS m^{-1}) as a result of incomplete surface mixing following a rainfall event that had occurred the previous day. The

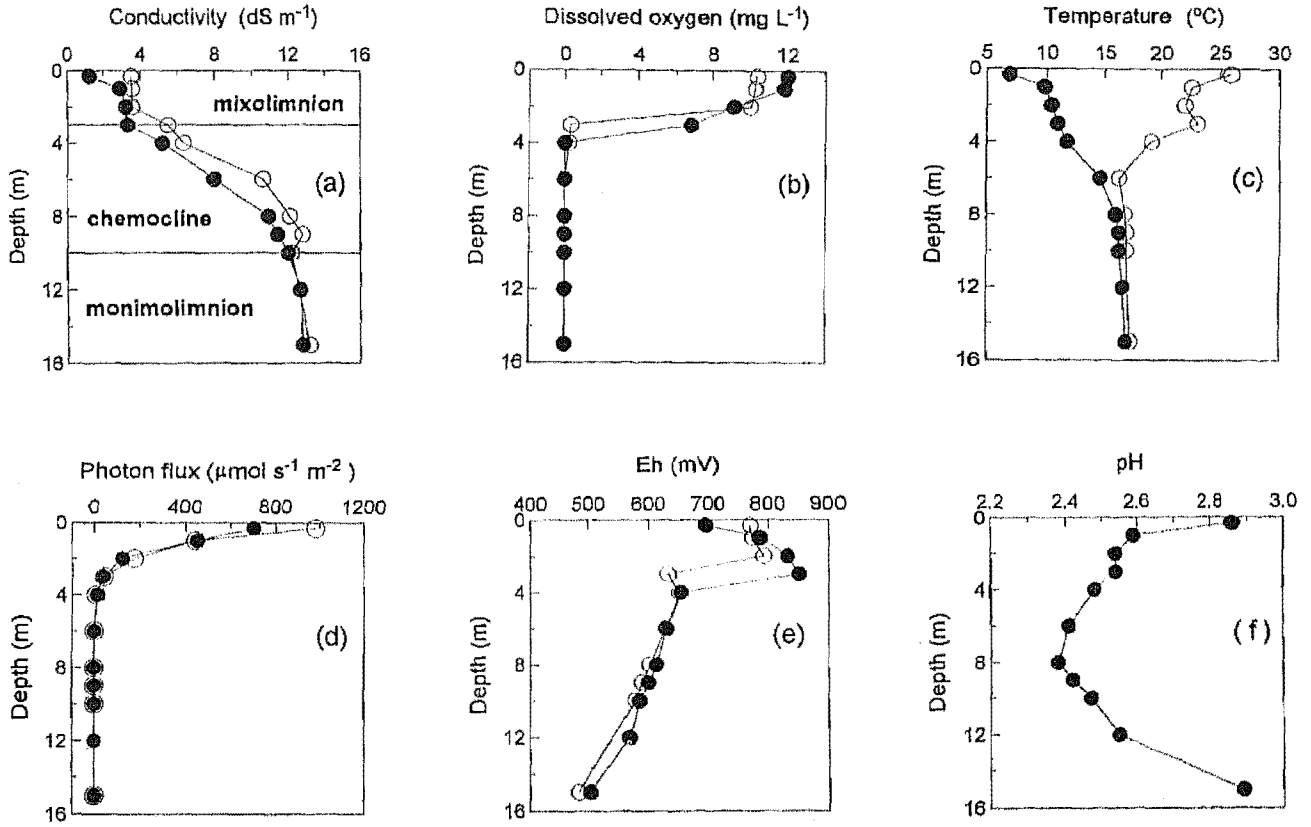

Fig. 3. Selected chemical and physical properties of the Spenceville Pit waters. *Open circles* = 31 Aug. 1994 (summer); *closed circles* = 28 Dec. 1994 (winter). Data points corresponding to depths of 0.3, 1, 2, 3, 4, and 8 m represent the means from Sampling Locations A and B. Precisions of the analyses were: specific conductance (±3%), dissolved O_2(g) (±5%), temperature (±1°C), Eh (±5 mV), and pH (±0.10 units).

similarity between the conductance profiles observed in the summer and winter indicates that the pit is probably permanently stratified (Fig. 3a).

The concentration of dissolved O_2(g) was highest in the surface waters, but decreased rapidly in the chemocline to produce an anoxic monimolimnion (Fig. 3b). The temperature profiles (Fig. 3c) show that the warmest and coldest temperatures were both observed at the pit surface (0.3 m) during summer and winter, respectively, and that seasonal oscillations are damped below a depth of approximately 8 m. The surface-water temperature was 19°C cooler in winter (Fig. 3c) and resulted in the higher dissolved O_2(aq) concentrations observed in winter at the lake surface (Fig. 3b) (Wetzel, 1983). Light penetration into the surface water was greatest in summer, but was absent below a depth of 4 m in both seasons (Fig. 3d).

The measured Eh values ranged from approximately 480 to 850 mV (Fig. 3e). The Eh at the surface was 75 mV lower in winter than in summer, and the values generally decreased with increasing depth. A 23-mV Eh increase in summer and a 163-mV Eh increase in winter was observed between the 0.30- and 4-m depths, relative to the surface. The pH values in the water column (Fig. 3f) decreased with increasing depth down to the lower chemocline, and increased thereafter in the monimolimnion, where the highest pH value in the water column was recorded (pH = 2.89). (Only pH values from the winter sampling are reported due to difficulties in electrode calibration during summer sampling.) Sulfide concentrations measured with the Ag/Ag_2S electrode were below the detectable limit (10^{-7} *M*).

The concentrations of dissolved C, P, and suspended particles generally increased with increasing depth in the water column (data not shown). The concentrations of DOC exhibited irregular trends with depth in the mixolimnion, ranging from 21.4 to 26.5 μmol L^{-1}. The DOC concentrations increased with increasing depth below this zone, however, and ranged from 137 μmol L^{-1} at the 4-m depth to 599 μmol L^{-1} at the 15-m depth. Phosphorus concentrations were 3.23 μmol L^{-1} in the mixolimnion and then increased with increasing depth below 3 m. In the chemocline, the P concentrations continued to increase from 10.7 to 14.5 μmol L^{-1}, and similar P concentrations were measured in the monimolimnion (12.3 μmol L^{-1}). Suspended particle concentrations were lowest in the mixolimnion (0.20–1.0 mg L^{-1}), increased in the chemocline (1.2–6.1 mg L^{-1}), and reached a maximum at the 15-m depth (26 mg L^{-1}).

The concentrations of the major and trace elements at each depth for each location are given in Table 1 (summer) and Table 2 (winter). Lead and Ba were below the detectable concentrations (2.4 and 3.6 μmol L^{-1}, respectively) in virtually all of the samples and thus these

Table 1. Selected chemical characteristics of the Spenceville Pit water samples collected on 31 Aug. 1994.

Depth	Eh	SO_4	Fe	(Fe^{2+}/Fe^{3+})†	Si	Al	Mg	Ca	Na	Cu	Mn	Zn	Ni	K
m	mV	mmol L^{-1}								μmol L^{-1}				
						Sampling Station A								
Mixolimnion														
0.3	757	20.3	2.72	0.085	1.59	2.53	4.48	4.42	1.02	0.563	117	379	2.44	38.9
1	790	20.3	2.69	0.023	1.61	2.53	4.44	4.29	1.04	0.573	122	399	2.40	44.3
2	790	20.4	2.71	0.023	1.70	2.60	4.40	4.29	1.06	0.565	119	393	2.50	34.3
3	617	42.4	12.3	14.2	1.65	5.23	7.98	5.84	1.20	1.38	169	589	5.52	3.58
Chemocline														
4	651	52.7	16.5	3.38	1.86	6.67	8.80	6.19	1.24	1.87	173	587	6.98	5.37
6	629	102	38.0	5.99	2.51	12.3	13.9	8.41	1.52	3.98	269	812	14.0	bd‡
8	604	128	53.0	14.1	2.64	14.9	17.6	9.38	1.64	4.03	357	1460	16.9	2.60
9	589	131	59.2	24.8	2.62	15.8	18.7	9.63	1.79	3.97	410	1760	21.6	bd
						Sampling Station B								
Mixolimnion														
0.3	782	20.5	3.84	0.036	1.63	2.57	4.57	4.42	1.09	0.568	135	445	3.07	35.8
1	757	19.5	2.96	0.088	1.62	2.59	4.36	4.34	1.05	0.527	125	422	3.20	51.2
2	795	21.0	2.81	0.018	1.58	2.45	4.40	4.47	1.06	0.524	120	444	3.71	58.8
3	647	44.0	12.7	4.32	1.69	5.11	7.94	5.94	1.16	1.29	186	606	7.14	30.7
Chemocline														
4	652	52.8	16.0	3.37	1.82	6.04	8.56	6.14	1.24	1.65	186	687	8.67	25.6
8	599	124	54.0	2.49	2.66	15.3	17.0	9.18	1.67	4.15	375	1460	20.3	10.2
10	579	136	63.5	16.1	2.77	16.0	19.3	9.71	1.81	3.74	462	1940	23.5	bd
Monimolimnion														
15	484	137	76.7	1400	2.10	14.2	22.1	9.66	2.82	1.60	464	2310	23.5	235

† Activity rato of Fe^{2+}(aq) to Fe^{3+}(aq) calculated from total dissolved Fe concentrations and Eh measurements using the geochemical speciation model MINTEQA2 (USEPA, 1991).
‡ bd = below detection = 2.60 μmol L^{-1} for K.

data are not included in Tables 1 and 2. The elemental concentrations show that the pit water chemistry is dominated by Fe, Al, Ca, Mg, and SO_4, and exhibits metal distributions similar to those reported for the Berkeley Pit (Davis and Ashenberg, 1989). The elemental profiles generally resemble the specific conductance profiles (Fig. 3a), with distinctly varying trends in the mixolimnion, chemocline, and monimolimnion. The data indicate that shortly after the addition of fresh waters from a winter rain, a 2-stratum mixolimnion is present, as shown by the dilution of the surface (0.3 m) metal concentrations in winter (Table 2) compared with summer (Table 1).

The existence of chemical stratification resulted in element concentrations and ionic strengths that increased with increasing depth in the water column. The dissolved constituents listed in Tables 1 and 2 represent ionic

Table 2. Selected chemical characteristics of the Spenceville Pit water samples collected on 28 Dec. 1994.

Depth	Eh	SO_4	Fe	(Fe^{2+}/Fe^{3+})†	Si	Al	Mg	Ca	Na	Cu	Mn	Zn	Ni	K
m	(mV)	mmol L^{-1}									umol L^{-1}			
						Sampling Station A								
Mixolimnion														
0.3	706	6.81	1.40	0.510	0.310	0.975	1.05	1.22	0.318	0.126	35.1	82.5	bd‡	49.1
1	779	16.8	2.80	0.021	1.39	1.94	3.44	3.22	0.831	0.400	96.7	265	bd	62.7
2	828	20.5	3.05	0.003	1.56	2.24	4.20	3.90	0.970	0.513	111	317	1.43	47.1
3	853	22.8	3.76	0.001	1.51	2.73	4.65	4.22	1.06	0.534	122	338	1.36	40.7
Chemocline														
4	658	33.7	10.3	2.41	1.65	4.26	7.40	5.50	1.19	1.04	159	424	2.59	36.1
6	630	83.1	27.6	10.6	2.21	9.60	12.1	7.41	1.48	2.75	244	794	5.67	25.8
8	614	116	48.0	8.54	2.46	14.4	16.1	9.11	1.68	4.25	330	1260	8.91	16.6
9	600	127	54.6	14.2	2.24	15.3	17.8	9.63	1.74	4.22	379	1680	10.5	25.3
						Sampling Station B								
Mixolimnion														
0.3	686	7.21	1.39	1.30	0.318	1.01	1.09	1.29	0.338	0.134	36.2	84.4	bd	45.0
1	793	18.6	2.52	0.011	1.33	1.95	3.69	3.49	0.987	0.442	97.6	274	bd	49.9
2	838	22.2	3.09	0.002	1.57	2.23	4.53	4.04	0.992	0.560	114	332	1.53	46.3
3	853	22.5	3.85	0.001	1.60	2.77	4.65	4.24	1.09	0.518	121	337	1.36	45.5
Chemocline														
4	652	39.7	10.7	2.74	1.71	4.41	7.53	5.61	1.24	1.18	169	448	2.91	31.0
8	614	123	48.0	8.10	2.44	14.4	15.9	9.08	1.70	4.39	335	1260	9.30	13.0
10	585	144	62.4	23.6	2.28	16.2	19.8	10.2	1.82	4.09	433	1910	11.3	22.8
Monimolimnion														
12	569	156	70.6	42.3	2.26	17.4	21.6	10.3	1.92	4.11	504	2390	14.1	17.1
15	504	169	85.0	520	2.05	16.9	24.3	10.9	2.29	2.66	584	2690	15.9	127

† Activity rato of Fe^{2+}(aq) to Fe^{3+}(aq) calculated from total dissolved Fe concentrations and Eh measurements using the geochemical speciation model MINTEQA2 (USEPA, 1991).
‡ bd = below detection = 1.30 μmol L^{-1} for Ni.

strengths ranging from 0.050 *M* in the mixolimnion (0.3-m depth) to 0.33 *M* in the monimolimnion (15-m depth). Ionic strengths in the dilute winter surface waters were 0.019 *M*. In the chemocline, the elemental concentrations increased with increasing depth, resulting in the increasing specific conductance values with increasing depth in this zone. The constituents Ca, Mn, Ni, and SO_4 behaved conservatively in the monimolimnion. In other words, their concentrations remained essentially constant between the lower chemocline and the mixolimnion, indicating no net loss or gain of these constituents in the deeper waters resulting from processes such as precipitation–dissolution, adsorption–desorption, or groundwater inflow–outflow. Sodium, Mg, Fe, K, and Zn concentrations, however, continued to increase with increasing depth in the mixolimnion. Copper, Al, and Si concentrations actually decreased between the upper and lower monimolimnion during both seasons.

Sediment Pore Fluid Chemistry

The Spenceville Pit sediment is unconsolidated and was determined to be approximately 60 cm in thickness, based on the difference between the depth at which the sediment sampler contacted the pit bottom and the depth at which sediment was collected with the cylindrical water sampler. The sediment Munsell color (wet) is 10R 4/4, or weak red. The elemental analysis of the sediment pore fluid, and the concentration of these elements relative to their concentrations near the sediment–water interface (15-m depth), are given in Table 3. The concentrations of Ca, Mg, Mn, Zn, Si, SO_4, and Ni in the pore fluid were virtually the same as their concentrations at the 15-m depth. The concentrations of Na, K, and Fe, however, were enriched in the pore water relative to concentrations at the 15-m depth. Aluminum and Cu concentrations continued to decrease across the sediment–water interface, as they did in the lower monimolimnion (Tables 1 and 2), resulting in lower pore water concentrations of Al and Cu relative to those at the 15-m depth (Table 3).

The porewater pH was 3.42, significantly higher than the monimolimnetic water (2.89), and the measured Eh was 509 mV. The calculated activity ratio of Fe^{2+}(aq) to Fe^{3+}(aq) was 396. Sulfide was detectable only in the pore fluid, with a concentration of 2.1×10^{-5} *M*. The concentration of DOC in the pore water was 9.49 mmol L^{-1}, significantly higher than that in the overlying water (0.60 mmol L^{-1}). Dissolved P concentrations in the pore water (11.6 μmol L^{-1}) were essentially the same as those in the monimolimnion.

Table 3. Selected chemical and physical properties of the Spenceville Pit sediment and pore water.

Component	Sediment†	Pore water‡	Relative pore water conc.§
Ca	146	10.9	1.00
Mg	1 530	24.9	1.03
Na	5 900	2.81	1.23
K	11 000	0.294	2.32
Fe	390 000	97.2	1.14
Al	24 000	15.3	0.91
Cu	840	1.78	0.67
Ni	<80	0.016	0.99
Mn	853	0.604	1.03
Zn	350	2.74	1.02
Si	446 000	2.08	0.99
S	390 000	161	0.96
pH	–	3.42	–
Eh	–	509 mV	–
Σ H_2S(aq)	–	2.1×10^{-5} *M*	–
Organic C	not measured	9.49 mmol L^{-1}	–

† Sediment concentrations in mg kg^{-1}. Concentration reported on a dry-wt. basis and corrected for the entrained pore fluid. The sediment was 54% H_2O on a dry wt. basis.
‡ Element concentrations are in mmol L^{-1}.
§ Value represents the concentration in the pore water relative to the concentration in the water column at the 15-m depth.

Sediment Mineralogy

The x-ray diffractograms of the Spenceville Pit sediment and the adjacent tailings revealed characteristic diffraction peaks corresponding to hematite (Fe_2O_3), quartz (α-SiO_2), and jarosite [$KFe_3(SO_4)_2(OH)_6$], and the x-ray patterns of the sediment and the adjacent mine tailings were essentially identical. The mineralogical composition of the sediment is consistent with the results obtained from the acid dissolution of sediment samples (Table 3). The data in Table 3 show that the sediment composition was dominated by Fe, S, K, and Si. The sediment also contained high concentrations of Al (2.4%), but the host phase for Al was not identified.

Geochemical Modeling

The results of the MINTEQA2 chemical speciation of the waters sampled in winter are presented in Table 4. Speciation data for the surface waters (0.3-m depth, Locations A and B), the lower mixolimnion (3-m depth, Locations A and B), the lower chemocline (10-m depth, Location B), the lower monimolimnion (15-m depth, Location B), and the pore water are presented. The calculations indicate that the speciation of Fe(III) is dominated by $FeSO_4^+$(aq), whereas Fe(II) exists primarily as Fe^{2+}(aq) in the mixolimnion and in the chemocline, and as $FeSO_4^+$(aq) in the monimolimnion and in the sediment pore water. In the surface waters, Al and Ca exist primarily as free ions, but the SO_4 complexes of Al and Ca become more abundant with increasing depth in the pit. The dominant orthophosphate species is $H_2PO_4^-$(aq). The majority of the P, however, is present as $FeH_2PO_4^{2+}$(aq) in the surface waters, mixolimnion, and chemocline, and as $FeH_2PO_4^+$(aq) in the monimolimnion and sediment pore water, consistent with the increasing proportions of Fe(II) to Fe(III) that were calculated for the lower depths and based on Eh measurements (Tables 1 and 2).

For the trace elements, the calculations indicate that the majority of the dissolved Cu, Ni, and Zn generally exists as free ions, and the remainder forms ion pairs with SO_4 (Table 4). The proportion of Cu and Ni complexed with SO_4 increased with increasing depth in the water column, reflecting the increased concentration of SO_4. The proportions of free and complexed metal ions are similarly distributed in the chemocline and the monimolimnion, and also in the sediment pore water. For Zn, the disulfate ion pairs became significant in the lower depths of the water column.

Table 4. Distribution of selected aqueous species and saturation indices for solid phases in the Spenceville Pit (winter profile) calculated using MINTEQA2.†

Parameter	Surface (0.3 m)	Mixolimnion (3 m)	Chemocline (10 m)	Monimolimnion (15 m)	Pore water
			Distribution of aqueous species		
Iron (III)					
% Fe^{3+}	13	10	6	5	5
% $FeOH^{2+}$	10	4	1	3	9
% $FeSO_4^+$	67	73	58	54	49
% $Fe(SO_4)_2^{2-}$	5	13	35	37	32
Iron (II)					
% Fe^{2+}	83	75	57	55	55
% $FeSO_4^0$	17	25	43	45	45
Aluminium					
% Al^{3+}	52	41	23	19	22
% $AlSO_4^+$	40	41	31	30	30
% $Al(SO_4)_2^-$	8	18	47	51	48
Calcium					
% Ca^{2+}	78	69	52	49	50
% $CaSO_4^0$	22	31	48	51	50
Phosphorus					
% $H_2PO_4^-$	12	5	10	16	13
% $FeH_2PO_4^+$	1	–	39	77	80
% $FeH_2PO_4^{2+}$	86	95	47	4	5
Copper					
% Cu^{2+}	78	68	51	48	50
% $CuSO_4^0$	22	32	49	52	50
Nickel					
% Ni^{2+}	80	70	52	50	52
% $NiSO_4^0$	20	30	47	50	48
Zinc					
% Zn^{2+}	75	63	35	32	34
% $ZnSO_4^0$	24	33	39	39	38
% $Zn(SO_4)_2^{2-}$	1	4	26	29	38
			Saturation indices for solid phases‡		
$AlOHSO_4$ (jurbanite)	−0.39	−0.21	+0.29	+0.69	+1.2
$KAl_3(SO_4)_2(OH)_6$ (alunite)	−2.6	−3.4	−3.1	−0.01	+3.6
$Fe(OH)_3$ (ferrihydrite)	−0.97	−1.5	−2.6	−2.6	−0.86
α-FeOOH (goethite)	+2.7	+2.4	+1.5	+1.6	+3.2
$CaSO_4 \cdot 2H_2O$ (gypsum)	−0.96	−0.27	+0.31	+0.35	+0.34
Fe_2O_3 (hematite)	+10	+9.8	+7.9	+8.1	+12
$KFe_3(SO_4)_2(OH)_6$ (jarosite)	+6.9	+7.4	+5.4	+5.1	+8.9
$FePO_4 \cdot 2H_2O$ (strengite)	+0.77	+0.08	+0.11	−0.24	+0.85
$SiO_2 \cdot nH_2O$ (amorphous)	+0.17	+0.25	+0.30	+0.24	+0.28
FeS (mackinawite)	−88	−110	−65	−57	−62
ZnS (sphalerite)	−82	−100	−61	−52	−57
CuS (covellite)	−69	−88	−48	−40	−45

† Data from surface and mixolimnion are averages from Locations A and B; data from chemocline and monimolimnion are from Location B.

‡ Saturation index = log (ion activity product[IAP]/solubility constant[K_{sp}]) for solid phases. Log (IAP/K_{sp}) > 0 indicates oversaturation of the respective solid phase. log (IAP/K_{sp}) < 0 indicates undersaturation of the solid phase.

The calculated SI values for jurbanite ($AlOHSO_4$) and alunite [$KAl_3(SO_4)_2(OH)_6$] are negative in the shallow waters, but the positive SI values calculated for the lower depths indicate that precipitation of these solids is thermodynamically possible (Table 4). The waters were undersaturated with respect to ferrihydrite [$Fe(OH)_3$] at all depths, but oversaturated with respect to the Fe-bearing phases goethite (α-FeOOH), hematite, and jarosite. Equilibrium conditions were calculated for gypsum ($CaSO_4 \cdot 2H_2O$) and amorphous silica ($SiO_2 \cdot nH_2O$) at all depths (Table 4) and for strengite ($FePO_4 \cdot 2H_2O$) in the mixolimnion, chemocline, and monimolimnion. Due to the low sulfide concentrations, extreme degrees of undersaturation were observed for mackinawite (FeS), sphalerite (ZnS), and covellite (CuS).

Water Balance Calculations

The results of the Spenceville Pit water-balance calculations indicate that the magnitude of the inflow components are surface runoff (1.35×10^7 L yr^{-1}), precipitation (1.70×10^6 L yr^{-1}), and groundwater inflow (9.35×10^5 L yr^{-1}). The magnitude of the dominant outflow components are direct evaporation from the water surface (2.78×10^5 L yr^{-1}) and groundwater outflow through the metavolcanic bedrock (4.42×10^5 L yr^{-1}). The remaining 1.29×10^7 L yr^{-1} represents the inflow that initially filled the Spenceville Pit. After the initial pit filling, the remaining inflow of 1.29×10^7 L yr^{-1} drains from the pit via surface water overflow and groundwater outflow through the terrace deposits that overlie the metavolcanic bedrock. From the known volume of the excavation (2.28×10^7 L), the initial filling of the Spenceville Pit was calculated to take approximately 2 yr, and thus the pit has been inundated for about 75 yr.

DISCUSSION

Development of Chemical Stratification

Chemical distributions in the water column of the Spenceville Pit are characteristic of a meromictic lake with poor mixing and significant chemical stratification. In a recent study of 260 lakes in North America, Anderson et al. (1985) cited (i) protection from wind-induced mixing and (ii) relative depths >5% as the most important factors contributing to the persistence of meromictic conditions. The relative depth of the Spenceville Pit is 34% and the pit waters are protected from wind mixing by the local topography. The inherent high relative depths of pit lakes, combined with the addition of acidic mine waters exhibiting high ionic strengths, predispose the waters to chemical stratification.

During the early stages of filling, ground and surface waters that entered the pit became concentrated through evaporation. The rain and surface waters that subsequently entered the pit were dilute relative to the existing pit waters, and the water column became chemically stratified as a result of density gradients and protection from wind-induced mixing. In winter, the addition of overland flow and rainwater results in a near-surface layer that is less dense than the deeper waters, and the presence of this 2-layer stratum is detectable through both the diluted shallow water metal concentrations measured in winter (Tables 1 and 2) and the specific conductance, Eh, and pH values in winter that indicate relatively dilute waters near the pit surface (Fig. 3a, 3e, and 3f). The existence of this two-layer stratum is only temporary, however, because sufficient wind energy exists to induce mixing of the upper 3 m of the pit water. The cycle of evaporation followed by dilution repeats each year,

resulting in deeper waters that are apparently sufficiently saline to offset the seasonal changes in density at the surface caused by heating and cooling. These processes result in chemical stratification of the water column that appears to be permanent; however, more frequent sampling would be necessary to assess the seasonal turnover of the Spenceville Pit.

Groundwater inflow to the Spenceville Pit is another process influencing the elemental profiles. The data in Tables 1 and 2 show that the relative increases in concentration with depth for elements that are expected to display conservative behavior (e.g., Na and Mg) are variable. For example, Table 1 shows that Na concentrations increase from a mean value of 1.06 mmol L^{-1} at the surface to 2.82 mmol L^{-1} at the bottom of the pit, or by a factor of 2.7. Magnesium concentrations, however, increase from a mean value of 4.53 mmol L^{-1} at the surface to 22.1 mmol L^{-1} at the pit bottom, or by a factor of 4.9. These observations indicate that groundwater inflow contributes to the observed elemental concentration profiles with depth in the Spenceville Pit, either by elemental additions (e.g., Mg) or by dilution (e.g., Na).

Chemical and Biological Processes in the Water Column

The chemical composition of the Spenceville Pit water is dominated by dissolved Fe, Al, Ca, Mg, and SO_4. The low pH values (<2.60) are typical of acid mine waters produced from the microbially catalyzed oxidation of sulfide minerals (e.g., pyrite) (Nordstrom, 1982a). The range in Eh values is within the range reported for the Berkeley Pit (Davis and Ashenberg, 1989) and falls within the category of mine waters that are in contact with the atmosphere, as described by Garrels and Christ (1965). Concentrations of DOC in the shallow waters of the pit range from 21.4 to 137 μmol L^{-1}, whereas the common range for DOC concentrations in natural lakes is approximately 170 to 830 μmol L^{-1} (Drever, 1988). Dissolved P concentrations in the mixolimnion (3.23 μmol L^{-1}), however, are typical of those commonly observed in freshwater lakes; below a depth of 3 m, they are quite elevated in comparison (10.7–14.5 μmol L^{-1}) (Faust and Osman, 1981; van der Leeden et al., 1990). Thus, photosynthetic activity appears to be limited in the pit water when compared with the majority of freshwater lakes, based on the relatively low DOC concentrations and the relatively high P concentrations observed. Undoubtedly, the high H ion concentrations and the elevated free metal ion concentrations result in conditions that are unfavorable for the growth of photosynthetic organisms.

Iron is an important constituent in the pit water because precipitated Fe hydroxides have the potential to scavenge trace metals from the water column as they precipitate and settle (Benjamin and Leckie, 1981; Sigg, 1985). Trace metal scavenging by suspended particulates, however, does not appear to be a significant factor controlling trace metal distributions in the Spenceville Pit, due to the low suspended particle concentrations observed and the low adsorption affinities of Cu and Zn at the pH ranges encountered (Benjamin and Leckie, 1981; Dzombak and Morel, 1990). This conclusion is also supported by the work of Schultz et al. (1987), who demonstrated complete metal desorption from ferrihydrite as the pH was decreased from 9.5 to 4.5. Davis and Ashenberg (1989) further concluded that scavenging of trace metals by amorphous Fe hydroxides in the Berkeley Pit was insignificant due to the acidic nature of the pit water.

The data in Tables 1 and 2 show that distributions of Ni and Zn in the water column are similar to those of the major ions, suggesting that the elemental profiles are controlled by the cyclic evaporation and filling and by the groundwater inputs, as discussed above. A decrease in soluble Cu concentrations, however, was observed between the lower chemocline and the sediment pore water (Tables 1, 2, and 3), but is difficult to explain on the basis of particle adsorption or precipitation. Geochemical calculations (MINTEQA2) show that the pit water is undersaturated with respect to several cupric minerals that are commonly associated with acid mine water in various geochemical environments (Alpers et al., 1994), e.g., covellite (CuS), antlerite [$Cu_3(SO_4)(OH)_4$], brochanite [$Cu_4(SO_4)(OH)_6$], and chalcanthite ($CuSO_4 \cdot 5H_2O$) (Table 4).

Table 4 shows that the waters were oversaturated with respect to goethite, although the slow growth kinetics of goethite probably result in metastable phases of ferrihydrite and microcrystalline goethite, which tend to be more common in acid-mine environments (Alpers et al., 1994; Bigham, 1994). Oxidation of Fe(II) in the shallow waters followed by precipitation of Fe(III) results in a net release of 2 moles of protons per mole of Fe, resulting in the lower pH values observed in the lower mixolimnion and chemocline (Fig. 3f):

$$Fe^{2+}(aq) + 1/4O_2(g) + H^+(aq) \rightarrow Fe^{3+}(aq) + 1/2H_2O(l) \quad [2]$$

$$Fe^{3+}(aq) + 2H_2O(l) \rightarrow \alpha\text{-}FeOOH(s) + 3H^+(aq) \quad [3]$$

The activity ratios of $Fe^{2+}(aq)$ to $Fe^{3+}(aq)$, calculated from Eh measurements and total dissolved Fe concentrations at each depth (Tables 1 and 2), are consistent with the processes of Fe oxidation and precipitation in shallow waters, as depicted above. The ratio of $Fe^{2+}(aq)$ to $Fe^{3+}(aq)$ in the shallow pit water was 15 times higher in winter compared with summer, reflecting recent inputs of $Fe^{2+}(aq)$ in winter surface runoff from the surrounding mine tailings. Oxidation of Fe(II) to Fe(III) resulted in a marked decrease in the ratio of $Fe^{2+}(aq)$ to $Fe^{3+}(aq)$ in the oxygenated lower mixolimnion when compared with the shallower waters. This trend was more pronounced in winter, and is illustrated by the increasing Eh measurements with depth in the mixolimnion (Fig. 3e).

Below the mixolimnion, an increase in the activity ratios of $Fe^{2+}(aq)$ to $Fe^{3+}(aq)$ with depth was observed (Tables 1 and 2). Although abiotic processes, such as ferric Fe precipitation, may act to increase the activity ratios of $Fe^{2+}(aq)$ to $Fe^{3+}(aq)$, this would not explain the increase in Fe(II) concentrations. A more plausible explanation for the decreasing Eh values in the water

column is based on the reduction of Fe(III) below the mixolimnion, coupled with oxidation of organic matter. The clinograde oxygen profile (Fig. 3b) is a distinct characteristic of permanently stratified, natural lakes, and is an indication of microbial activity that results in greater removal of oxygen by biological oxidation of organic matter than can be supplied by mixing of the shallow and deep waters (Wetzel, 1983; Balistrieri et al., 1994).

Utilization of soluble and particulate forms of Fe(III) as an electron acceptor in the oxidation of organic matter has been demonstrated by a diverse population of microorganisms, under a variety of conditions (Lovley, 1991):

$$4\ \alpha\text{-FeOOH(s)} + CH_2O(s) + 8H^+(aq) \rightarrow 4Fe^{2+}(aq) + CO_2(g) + 7H_2O(l) \quad [4]$$

The consumption of protons and production of Fe(II) illustrated in Eq. [4] are consistent with trends in decreasing Eh and increasing pH that were observed near the bottom of the pit (Fig. 3e and 3f), where particle concentrations were highest. The increasing pH values with depth in the monimolimnion (Fig. 3f) and in the pore water (Table 3) are also indicative of bacterial SO_4 reduction, a process that results in the production of alkalinity and the incorporation of S as inorganic forms in sediments affected by acid mine drainage. The measurable sulfide concentrations in the sediment pore water (Table 3) provide further evidence of biological transformations of Fe and S near the bottom of the pond.

A high degree of jarosite oversaturation was calculated in the Spenceville Pit at all depths (Table 4). This mineral is ubiquitous in acid-mine environments, where conditions of oversaturation are commonly observed (Nordstrom, 1982a; Jambor, 1994). Although kinetic barriers may act to slow the precipitation of jarosite in the pit waters (Alpers et al., 1994), jarosite was identified by XRD analysis of the tailings and bottom sediments. The equilibrium conditions calculated for strengite also indicate that it is a solid phase that may potentially control P concentrations.

Elevated Al concentrations in the Spenceville Pit most likely result from the enhanced dissolution of aluminosilicate minerals as a result of their contact with the acidic waters (Nordstrom, 1982b). Saturation indices representative of equilibrium conditions were calculated for alunite in the monimolimnion, and for jurbanite in the mixolimnion and the chemocline (Table 4), indicating the potential for these minerals in controlling Al solubility. Nordstrom (1982b) also implicates basaluminite [$Al_4(SO_4)(OH)_{10} \cdot 5H_2O$] as a possible solid phase that may control Al solubilities in acid mine environments. Basaluminite, however, is metastable with respect to the above-mentioned Al minerals, and the data for this study lie below the solubility line for basaluminite in the diagram provided by van Breeman (1973). The SI values for jurbanite and alunite at the 15-m depth (Table 4) indicate near-equilibrium conditions between the two minerals, but they were not identified in the sediments by XRD analysis. Sediment analyses, however, indicate that Al comprises 2.4% of the sediments by weight, and that S is also a significant component (3.9%) of the sediment. In addition, pore water S and Al concentrations indicate a net loss of these elements relative to the 15-m depth (Table 3). These observations suggest that jurbanite is the likely phase that controls Al solubility in the Spenceville Pit. Jurbanite was also implicated as an Al solubility control in the Berkeley Pit (Davis and Ashenberg, 1989).

The Spenceville Pit waters were calculated to be at equilibrium with respect to gypsum in the mixolimnion (Table 4). In addition to goethite and jarosite, gypsum is one of the most abundant secondary minerals found in sulfide-rich tailings impoundments (Jambor, 1994). Although gypsum equilibrium was calculated in the Spenceville Pit, the characteristic XRD peaks for gypsum were not identified in the sediments; in addition, sediment Ca concentrations were low (<0.02%) (Table 3) and the concentrations of dissolved Ca remained constant throughout the monimolimnion and into the interstitial water (Tables 1, 2, and 3). Based on the equilibrium conditions observed, gypsum precipitation may act to control Ca concentrations in the Spenceville Pit waters.

CONCLUSIONS

A detailed study of the Spenceville Pit water column indicates that certain chemical properties and mineral solubility controls operate that are unique to acidic pit lakes. Striking similarities in the pH, redox state, mineral saturation states, and concentration profiles of the major and trace elements exist in comparison with the Berkeley Pit at Butte, MT, though on a much smaller scale. The minerals gypsum, goethite, jarosite, and jurbanite were identified as solids that may control metal solubility in the Spenceville Pit waters.

Unlike natural, higher pH lakes, where scavenging of trace metals by particulate Fe hydroxides can be significant, trace metal distributions in acidic pit lakes are more often controlled by the processes of seasonal filling and evaporation. These processes, coupled with the inherent high relative depths of pit lakes, predispose the pit lakes to chemical stratification. High salinities are produced by evapoconcentration of the pit water, and this eventually results in the genesis of deeper waters that are sufficiently dense to offset seasonal changes in density at the surface caused by heating and cooling. These observations are consistent with our current understanding of the relationships between physical dimensions and stratification of pit lakes.

Other physical and geochemical processes that occur in acidic pit lakes are not unique to these environments but may operate in natural, higher pH lakes as well. Water column profiles of specific conductance, dissolved oxygen, and temperature in acidic pit lakes are characteristic of a meromictic lake that exhibits poor mixing. The data from this study suggests that microbial oxidation of organic C is coupled with Fe(III) reduction in water below the zone of mixing, where dissolved $O_2(g)$ is absent. In an analogous fashion to natural lakes, this process results in reducing conditions in monimolimnetic waters. The combination of high Fe(III) and low organic

C concentrations in pit lakes, however, limits the extent of SO_4 reduction. Thus, sulfide concentrations are low, precluding the quantitative precipitation of trace metals as diagenetic metal sulfides.

ACKNOWLEDGMENTS

Special thanks are extended to Adam E. Cosner and Mike Lacy for their assistance with field sampling. We would also like to express appreciation to D.D. Runnells, A. Herlihy, M.A. Williamson, D.R. Parker, and W.C. Bennett for the time and effort spent reviewing this manuscript. This research was funded, in part, by grants from the California Department of Conservation, Interagency Agreement no. 4093-529, and from the National Science Foundation (EAR 9302069).

REFERENCES

Alpers, C.N., D.W. Blowes, D.K. Nordstrom, and J.L. Jambor. 1994. Secondary minerals and acid mine-water chemistry. p. 247–270. *In* J.L Jambor and D.W. Blowes (ed.) The environmental chemistry of sulfide-mine wastes. Short course notes, Vol. 22. Mineralogical Assoc. of Canada, Nepean, ON.

American Public Health Association. 1992. Standard methods for the examination of water and wastewater. 18th ed. APHA, Washington, DC.

Anderson, R.Y., W.E. Dean, J.P Bradbury, and D. Love. 1985. Meromictic lakes and varved sediments in North America. U.S. Geol. Surv. Bull. 1607.

Aubury, L.E. 1908. The copper resources of California. Bull. Calif. Div. Mines Geol. 50.

Balistrieri, L.S., J.W. Murray, and B. Paul. 1994. The geochemical cycling of trace elements in a biogenic meromictic lake. Geochim. Cosmochim. Acta 58:3993–4008.

Ball, J.W., and D.K. Nordstrom. 1985. Major and trace element analyses of acid mine waters in the Leviathan mine drainage basin, California/Nevada, October 1981 to October 1982. Water Resour. Invest. (U.S. Geol. Surv.) 85-4169.

Benjamin, M.M., and J.O. Leckie. 1981. Multiple-site adsorption of Cd, Cu, Zn, and Pb on amorphous iron hydroxide. J. Colloid Interface Sci. 79:209–221.

Bigham, J.M. 1994. Mineralogy of ochre deposits formed by sulfide oxidation. p. 103–132. *In* D.W. Blowes and J.L Jambor (ed.) The environmental chemistry of sulfide mine wastes. Mineralogical Assoc. of Canada, Waterloo, ON.

Bird, D.A., W.B. Lyons, and G.C. Miller. 1994. An assessment of hydrogeochemical computer codes applied to modeling post-mining pit water geochemistry. p. 31–40. Proc. of the First Int. Conf. on Tailings and Mine Waste, Fort Collins, CO. 19–21 Jan. 1994. A.A. Balkema, Rotterdam.

Bradley, W.W. 1930. Report XXVII of the State Mineralogist. California Div. of Mines. California State Print. Office, Sacramento, CA.

California Department of Water Resources. 1981. California rainfall summary, monthly total precipitation, 1849–1980. Calif. Dep. of Water Resour., Sacramento, CA.

Davis, A., and D. Ashenberg. 1989. The aqueous geochemistry of the Berkeley Pit, Butte, Montana, U.S.A. Appl. Geochem. 4:23–69.

Doyle, G.A. 1996. Physical limnology of existing pit lakes. Presented at the Society for Mining, Metallurgy, and Exploration, Inc. Annu. Meeting, Phoenix, AZ. 11–14 Mar. 1996. Preprint 96-75. Soc. for Mining, Metallurgy, and Exploration, Inc. Littleton, CO.

Drever, J.I. 1988. The geochemistry of natural waters. 2nd ed. Prentice Hall, Englewood Cliffs, NJ.

Dzombak, D.A., and F.M.M. Morel. 1990. Surface complexation modeling. John Wiley & Sons, New York.

Faust, S.D., and M.A. Osman. 1981. Chemistry of natural waters. Ann Arbor Science Publ., Ann Arbor, MI.

Garrels, R.M., and C.L. Christ. 1965. Solutions, minerals, and equilibria. Freeman, Cooper, and Co., San Francisco, CA.

Haan, C.T., B.J. Barfield, and J.C. Hayes. 1994. Design hydrology and sedimentology for small catchments. Academic Press, San Diego, CA.

Jackson, M.L. 1979. Soil chemical analysis. Advanced course. 2nd ed. M.L. Jackson, Madison, WI.

Jambor, J.L. 1994. Mineralogy of sulfide-rich tailings and their oxidation products. p. 59–102. *In* J.L Jambor and D.W. Blowes (ed.) The environmental chemistry of sulfide-mine wastes. Short course notes, Vol. 22. Mineralogical Assoc. of Canada, Nepean, ON.

Joint Committee on Powder Diffraction Standards. 1993. Mineral powder diffraction file databook. JCPDS, Swarthmore, PA.

Levy, D.B., K.H. Custis, W.H. Casey, and P.A. Rock. 1997. A comparison of metal attenuation in mine residues and overburden material from an abandoned copper mine. Appl. Geochem. (in press).

Lim, C.H., and M.L. Jackson. 1982. Dissolution for total elemental analysis. p. 1–12. *In* A.L. Page et al. (ed.) Methods of soil analysis. Part 2. 2nd ed. ASA, and SSSA, Madison, WI.

Lovley, D.R. 1991. Dissimilatory Fe(III) and Mn(IV) reduction. Microbiol. Rev. 55:259–287.

Lyons, W.B., G.A. Doyle, R.C. Peterson, and E.E. Swanson. 1994. The limnology of future pit lakes in Nevada: The importance of shape. p. 245–248. *In* Proc. of the First Int. Conf. on Tailings and Mine Waste, Fort Collins, CO. 19–21 Jan. 1994. A.A. Balkema, Rotterdam.

Miller, G.C., W.B. Lyons, and A. Davis. 1996. Understanding the water quality of pit lakes. Environ. Sci. Technol. 30:118–123.

Nordstrom, D.K. 1982a. Aqueous pyrite oxidation and the consequent formation of secondary iron minerals. p. 37–56. *In* J.A. Kittrick et al. (ed.) Acid sulfate weathering. SSSA Spec. Publ. 10. SSSA, Madison, WI.

Nordstrom, D.K. 1982b. The effect of sulfate on aluminum concentrations in natural waters: Some stability relations in the system Al_2O_3–SO_3–H_2O at 298 K. Geochim. Cosmochim. Acta 46:681–692.

Nordstrom, D.K., E.A. Jenne, and J.W. Ball. 1979. Redox equilibria of iron in acid mine waters. *In* E.A. Jenne (ed.) Chemical modeling in aqueous systems. ACS Symp. Ser. 93:51–79.

Pillard, D.A., T.A. Doyle, D.D. Runnells, and J. Young. 1996. Post-mining pit lakes: Predicting lake chemistry and assessing ecological risks. Proc. of the 3rd Int. Conf. on Tailings and Mine Waste, Fort Collins, CO. 16–19 Jan. 1996. A.A. Balkema, Rotterdam.

Pruitt, W.O., and R.L. Snyder. 1985. Crop water use. p. 5-1 to 5-49. *In* G.S. Pettygrove and T. Asano (ed.) Irrigation with reclaimed municipal wastewater—a guidance manual. Lewis Publ., Chelsea, MI.

Raue, B., H.J. Brauch, and F.H. Frimmel. 1991. Determination of sulphate in natural waters by ICP/OES—comparative studies with ion chromatography. Fresenius Z. Anal. Chem. 340:395–398.

Schultz, M.F., M.M Benjamin, and J.F. Ferguson. 1987. Adsorption and desorption of metals on ferrihydrite: Reversibility of the reaction and sorption properties of the regenerated solid. Environ. Sci. Technol. 21:863–869.

Sigg, L. 1985. Metal transfer mechanisms in lakes; the role of settling particles. p. 283–310. *In* W. Stumm (ed.) Chemical processes in lakes. John Wiley & Sons, New York.

Singer, P.C., and W. Stumm. 1970. Acidic mine drainage: The rate determining step. Science (Washington, DC) 167:1121–1123.

Sung, W., and J.J. Morgan. 1980. Kinetics and products of ferrous iron oxygenation in aqueous systems. Environ. Sci. Technol. 14: 561–568.

Theisen, A.A., and M.E. Harward. 1962. A paste method for preparation of slides for clay mineral identification by x-ray diffraction. Soil Sci. Soc. Am. Proc. 26:90–91.

U.S. Environmental Protection Agency. 1991. MINTEQA2/PRODEFA2, a geochemical assessment model for environmental systems: Version 3.0 users manual. USEPA Rep. 600/3-91/021. Center for Exposure Assessment and Modeling, Office of Res. and Dev., Environ. Res. Lab, Athens, GA.

van Breeman, N. 1973. Dissolved aluminum in acid sulfate soils and in acid mine waters. Soil Sci. Soc. Am. Proc. 37:694–697.

van der Leeden, F., F.L. Troise, and D.K. Todd. 1990. The water encyclopedia. 2nd ed. Lewis Publ., Chelsea, MI.

Wetzel, R.G. 1983. Limnology. 2nd ed. Saunders College Publ., Philadelphia.